Quantification of the Hepatitis B Virus cccDNA: Evidence-based guidelines for monitoring the key obstacle of HBV cure

Short Title: cccDNA quantification harmonization

Lena Allweiss[1,2], Barbara Testoni[3,4], Mei Yu[5], Julie Lucifora[3,4], Chunkyu Ko[6*], Bingqian Qu[7**], Marc Lütgehetmann[8,2], Haitao Guo[9,10], Stephan Urban[7,2], Simon P. Fletcher[5], Ulrike Protzer[6,2], Massimo Levrero[3,4], Fabien Zoulim[3,4], Maura Dandri[1,2]

1. I. Medical Clinic and Polyclinic, University Medical Center Hamburg-Eppendorf, Hamburg, Germany
2. German Center for Infection Research (DZIF), Germany
3. Cancer Research Center of Lyon, INSERM U1052, Lyon, France
4. ANRS AC34
5. Gilead Sciences, Foster City, California, United States of America
6. Institute of Virology, Technical University of Munich, Munich, Germany
* Current affiliation: Infectious Diseases Therapeutic Research Center, Therapeutics & Biotechnology Division, Korea Research Institute of Chemical Technology (KRICT), 34114 Daejeon, Republic of Korea
7. Department of Infectious Diseases, Molecular Virology, University Hospital Heidelberg, Germany
** Current affiliation: Division of Veterinary Medicine, Paul Ehrlich Institute, Germany
8. Institute of Medical Microbiology, Virology and Hygiene, University Medical Center Hamburg-Eppendorf Hamburg, Germany
9. Indiana University School of Medicine, Indianapolis, Indiana, United States of America
10. Current affiliation: Department of Microbiology and Molecular Genetics, Cancer Virology Program, UPMC Hillman Cancer Center, University of Pittsburgh School of Medicine, Pittsburgh, United State of America

Table of contents

Allweiss L, *et al. Gut* 2023; 72:972–983. doi: 10.1136/gutjnl-2022-328380

Supplementary material and methods

Generation, infection, treatment and viral characterization of human liver chimeric. All animal experiments were performed in accordance with the European Union directive 2010/63/EU and approved by the ethical committee of the city and state of Hamburg in accordance with the ARRIVE guidelines. The generation of USG (uPA/SCID/beige/IL2RG-/-) mice reconstituted with human hepatocytes was conducted as previously reported[1]. HBV infection was established upon a single intraperitoneal injection of HBV-containing USG mouse serum (1x10^7 HBV DNA copies/mouse, genotype D, HBeAg-positive). Blood samples were taken retro-orbitally during the experiments. Viral DNA was extracted from serum samples using the QiAamp MinElute Virus Spin Kit (Qiagen, Hilden, Germany) and quantified with HBV-specific primers and probes (TaqMan® Gene Expression assay ID: Pa03453406_s1). HBV core antigen on cryostat liver sections was visualized by immunofluorescence staining as described earlier[1]. Some mice received Lamivudine (Lam) (Epivir, ViiV Healthcare, Zeist, Netherlands) for six or 12 weeks supplemented in the drinking water (20mg/100ml).

HBV infection and preparation of HepG2-NTCP cell culture samples. HepG2-NTCP cells were cultured and infected as described elsewhere[2]. Briefly, cells were infected with HepAD38-derived virus (genotype D) at an MOI of 100 genome equivalents (GE) / cell and harvested at day 9 post infection. The cells were pooled before being divided and shipped to the four participating labs. Every lab received a frozen cell pellet of approximately 1x10^7 cells, which upon arrival was dissolved in 900 µl 10 mM Tris-HCl / 10 mM EDTA buffer and distributed equally for the three DNA extractions. HepG2-NTCP cells for the SB in **Figure 4F** were infected with an MOI of 250 GE / cell and harvested at day 9 post infection as described elsewhere[3]. For **Supplementary Figure 7**, HepG2-NTCP cells were generated by transfection of expression vector pEF1/v5-His-B (Thermo Fisher Scientific) encoding the human NTCP human into HepG2 cells (ATCC). Transfected HepG2 cells were selected with G418 at 1 mg/ml for 3 weeks and the G418-resistant colonies expanded and tested for NTCP functional activity by monitoring uptake of tritium labeled taurocholate (3H(G)]-taurocholic acid 250 µCi, 9.25MBq, Perkin Elmer). Cells were infected with an MOI of 4000 GE / cell.

Alkaline Hirt DNA extraction. HBV cccDNA was extracted from HBV-infected humanized mouse liver tissue and HepG2-NTCP cells with a modified Hirt DNA extraction method as described previously[4,5]. Cell lysis in an alkaline milieu irreversibly denatures genomic DNA and all non-cccDNA HBV DNA species. After rapid neutralization, only supercoiled cccDNA renatures and remains in the supernatant after centrifugation. Briefly, 6x10^6 cells or 10mg liver tissue were diluted and homogenized in 400µl 10mM Tris-HCl (pH 7.5)/10mM EDTA (pH 8.0)/0.2% NP40. Cell lysis was achieved by the addition of 400µl 6%SDS/0.1M NaOH and 30min incubation at 37°C with agitation. The alkaline lysate was neutralized by the addition of 200µl of 3M potassium acetate (pH 4.8) and centrifuged for 15 min at 4°C and 14,500g. The supernatant was extracted with phenol (pH>7.2) followed by an additional extraction with phenol/chloroform/isoamyl alcohol (25:24:1). The DNA was precipitated with isopropanol, pelleted by centrifugation, washed twice in 70% ethanol and dissolved in 10mM Tris-HCl/1mM EDTA buffer.

Nuclease digestions. The plasmid-safe ATP-dependent DNase (PSD)[6] selectively hydrolyses linear dsDNA and with a lower efficiency single-stranded DNAs (ssDNA). Notably, it does not affect nicked circular dsDNAs (with a single discontinuous strand). PSD also digests virion-derived rcDNA[6] and intracellular capsid-associated rcDNA[7] but not rcDNA after Hirt DNA extraction[7–9]. The T5 exonuclease is a dsDNA-specific exonuclease with ssDNA-specific endonuclease activity[9] and in contrast to PSD also acts on nicked dsDNA. This bears the risk

of degrading transcriptionally active cccDNA forms that must be temporarily nicked[10]. Exonuclease I catalyzes the removal of nucleotides from linear ssDNA, while exonuclease III removes nucleotides from linear or nicked dsDNA. Together, both enzymes remove HBV RI, but leave closed single and double strands undigested[11,12].

Unless otherwise indicated, the same amount of initial starting material was used for all downstream nuclease digestion and PCR analyses to enable a direct comparison of all settings within and among the participating labs. The nuclease digestion assays were run in independent duplicates. The DNA content was determined with the Qubit™ dsDNA BR Assay Kit (Thermo Fisher Scientific) and approximately 100ng or 500ng DNA from HepG2-NTCP or mice, respectively, was used for all the following conditions: "PSD low"[6]: 10U PSD (Lucigen), 2µl 25 mM ATP, 2µl of the proprietary reaction buffer, and water for a total volume of 20 µl; incubation at 37°C for 6h, heat inactivation at 70°C for 30 min. "PSD high"[1]: 30U PSD (Lucigen), 8µl 25 mM ATP, 20 µl of the proprietary reaction buffer, and water for a total volume of 200 µl; incubation at 37°C for 2 h, heat inactivation at 70°C for 30 min. "T5"[9]: 10U T5 exonuclease (T5; NEB, Ipswich, MA, USA), 2 µl NEB reaction buffer 4, and water for a total volume of 20 µl; incubation at 37°C for 45 min, heat inactivation at 70°C for 30 min. "T5 low"[2]: 5U T5, 2µl NEB reaction buffer 4, and water for a total volume of 20µl; incubation at 37°C for 30 min, heat inactivation at 70°C for 30 min. "Exo I/III"[11,12]: 20U exonuclease I (Exo I; NEB), 25U exonuclease III (Exo III; NEB), 2µl cutsmart™ buffer (NEB), and water for a total volume of 20µl; incubation at 37°C for 2h, heat inactivation at 80°C for 20 min. Digested and nondigested samples were column-purified using the Genomic DNA Clean & Concentrator™-25 (Zymo Research, Irvine, CA, USA) before downstream analyses. In preparatory studies, the effect of heat denaturation on PSD digestion efficiency was tested in several sample types. HBV-infected HepG2-NTCP cells, rcDNA extracted from infectious mouse serum and an HBV DNA containing plasmid as a cccDNA surrogate mixed with DNA from an uninfected humanized mouse liver were used. Before digestion with PSD low and high conditions, the input DNA (500ng) was denatured by 5 min incubation at 85°C.

Quantitative PCR measurements. Quantitative PCR measurements were performed using Taqman™ chemistry and the Taqman™ Fast Advanced Master Mix (Thermo Fisher Scientific). PCR was run in triplicates. cccDNA was quantified with cccDNA-selective primers and probe as published previously[13] using improved PCR conditions (final concentration of forward primer 100 nmol/l; reverse primer 800 nmol/l; cycling conditions: 10 min initial denaturation at 95°C followed by 40 cycles of 95°C for 1 sec and 65°C for 1 min)[14] (**Supplementary Fig. 2B**). Total HBV DNA was quantified with primer and probe from the Taqman™ Gene Expression System (assay ID: Pa03453406_s1; Thermo Fisher Scientific). This assay was tested against 16 HBV isolates including genotypes A, B, C, D, E, and G as per manufacturer's specifications. The final concentration of both primers was 250 nmol/l; cycling conditions were: 20 sec initial denaturation at 95°C followed by 40 cycles of 95°C for 1 sec and 65°C for 20 sec. Known amounts of an HBV DNA plasmid were amplified to establish a standard curve for absolute quantification of cccDNA and total HBV DNA. For the absolute quantification of cccDNA in gel-extracted DNA (**Fig. 3C**), digital droplet PCR (ddPCR) was employed. Template DNA, the same primers and probe as above were diluted in ddPCR Supermix for Probes (Biorad, Feldkirchen, Germany) to the same final concentration as above. After droplet generation and PCR (cycling conditions: 10 min initial denaturation at 95°C followed by 40 cycles of 94°C for 30 sec and 65°C for 1 min), droplets were analyzed on a QX100 droplet reader (Biorad). The sensitivity of the cccDNA-selective ddPCR assay has been determined elsewhere[15]. Viral DNA was normalized to the number of human cells by measuring the human single copy gene hemoglobin beta (assay ID Hs00758889_s1) or to mitochondrial DNA by measuring the human

mitochondrial gene ND2 (assay ID #Hs02596874_g1). Human genomic DNA (Roche Applied Science, Mannheim, Germany) was used to establish a standard curve for quantification.

Preparative agarose gel electrophoresis. Total DNA extracted without proteinase K was loaded on a 1.2% TAE agarose gel. After gel electrophoresis at 25 V for 21 h, all the upper and lower HBV DNA bands were excised separately by comparison to a 1 Kb DNA ladder (Thermo Fisher Scientific). DNA was extracted from the gel with the help of the QIAquick gel extraction kit (Qiagen) following the manufacturer´s instructions. The extracted DNA was analyzed by ddPCR as described above. For comparison, a SB was prepared with equal amounts of the same samples and run in parallel. Because liver samples from three different chimeric mice were used for this assay, samples had to be normalized to the degree of human repopulation in order to compare viral loads across mice. This was done by qPCR measurements of human mitochondrial DNA (via ND2) in the undigested samples and loading of normalized amounts on the gel.

Southern blot analyses. SB analysis was performed as previously described[14,16]. Briefly, DNA was separated on an agarose gel and blotted on a Nytran membrane using downward capillary transfer. HBV DNA was detected with the help of branched DNA (bDNA) technology using the QuantiGene Singleplex assay (Thermo Fisher Scientific) and a full genome HBV probe (assay ID #VF1-12525). A detailed version of this protocol can be found on the ICE-HBV protocol database (https://ice-hbv.org/protocol/a-sensitive-and-rapid-southern-blot-assay-based-on-branched-dna-technology-for-the-detection-of-hbv-dna-in-cell-culture-and-liver-tissue-samples/).

Allweiss L, *et al. Gut* 2023; 72:972–983. doi: 10.1136/gutjnl-2022-328380

Supplementary results

Impact of DNA quality on cccDNA quantification

While Hirt and -PK DNA extractions were sufficient to remove replicative intermediates to a degree that makes it possible to specifically detect cccDNA (including pf-rcDNA) in low replicative samples (NA treatment), nuclease digestion was still needed in highly infected samples to remove the “upper band”. However, nuclease treatment bears some risks and should be employed with caution. First, throughout the cross-validation experiments, we observed high variations in terms of digestion efficiency between the labs and even between replicates within one lab (data not shown). Second, excessive digestion conditions could lead to over-digestion of cccDNA. We therefore compared the standard “PSD high” and “T5” conditions used throughout this study with conditions where enzymatic units were increased by 4-fold and the incubation time was extended to 6 hours (T5-augmented). The SB and densitometric analysis of the cccDNA band in -PK extracted DNA from infected mouse liver tissue shows unaltered cccDNA levels with either PSD conditions, but 2-fold lower cccDNA levels after T5-augmented conditions (**Supplementary Fig.8A**). Although the chosen conditions were extreme, these results indicate that extended digestion conditions may become detrimental when using the T5 exonuclease. In an attempt to make the pf-rcDNA accessible to digestion by PSD, we included a heat denaturation step prior to “PSD low” and “PSD high” digestion reactions[8]. Heat denaturation increased the digestion efficiency of rcDNA derived from mouse serum (**Supplementary Fig.8B**) because the enzyme could then act on the denatured single strands. However, this experiment created the highest variations and appeared to digest nicked cccDNA because of its separation into single strands. Indeed, we could observe a much stronger reduction of the cccDNA PCR counts of an HBV DNA plasmid and HBV-infected HepG2-NTCP cells using PSD and heat denaturation compared to PSD alone, indicating that the plasmid preparation contained nicks. Because of this concern and the additional need to experimentally adapt the heat denaturation conditions to the amount and viscosity of the DNA sample, this approach did not prove to be advantageous over the other conditions described here for a PCR-based cccDNA quantification.

A common characteristic of all tested nucleases is their ability to hydrolyze linear or open DNA molecules but spare covalently closed circular forms from digestion. Thus, the quality of the extracted DNA is of utmost importance. Any condition provoking nicking of the cccDNA will make it a template for T5 exonuclease and exonuclease III, but not for PSD, while all enzymes (except exonuclease I) will act on damaged cccDNA containing double strand breaks. We occasionally obtained low quality DNA with detrimental effects on cccDNA measurements after nuclease digestions. **Supplementary figure 8C** serves as an example for accidental nicking showing two independent -PK DNA extractions from the same mouse liver tissue. In one of the extracts, however, the SB revealed a prominent “slow-migrating” band and only a faint “fast-migrating” band, indicating that the cccDNA was nicked and migrated as a relaxed circular form during electrophoresis. Notably, cccDNA measurement by qPCR was still possible using PSD treatment. **Supplementary figure 8D** shows an example of -PK extracted DNA that was severely damaged, containing nicks and double-strand breaks. By comparison to the high-quality -PK extracts in the cross-validation, this sample showed 0.6log lower cccDNA levels after digestion with all nucleases. Mitochondrial DNA was reduced by 2.1log on average during all nuclease digestions demonstrating damage of this circular DNA species as well.

Allweiss L, *et al. Gut* 2023; 72:972–983. doi: 10.1136/gutjnl-2022-328380

Supplementary figures

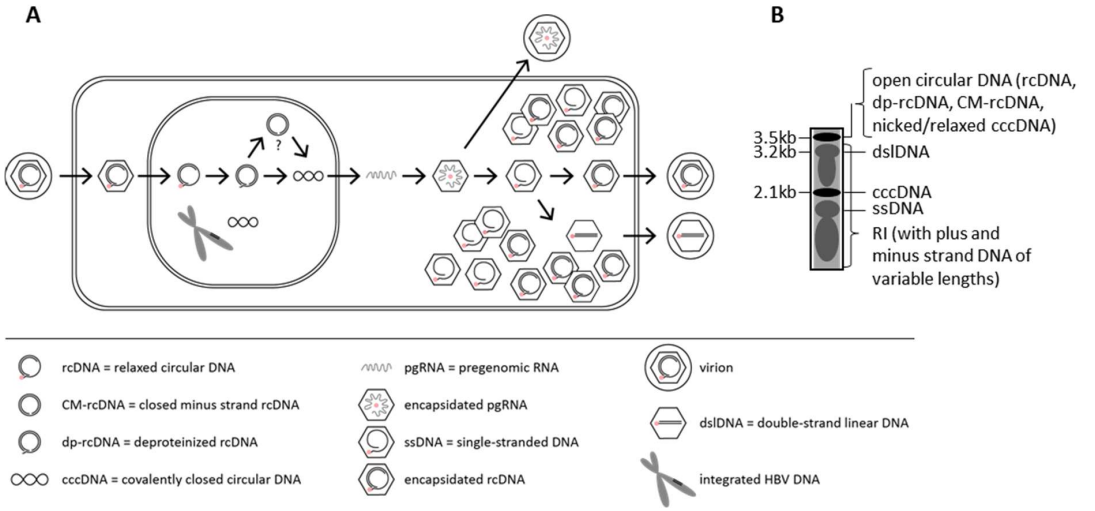

Supplementary figure 1: (**A**) Simplified HBV life-cycle with a focus on HBV DNA forms present in the cell. The pf-rcDNA is also known as dp-rcDNA. The removal of the viral polymerase might occur in the cytoplasm or the nucleus. The CM-rcDNA is a putative intermediate between pf-rcDNA and cccDNA. The encapsidated replicative intermediates occur with variable lengths of minus and plus strand DNA; however, only the defined intermediates i.e. pregenomic RNA, single-stranded DNA and relaxed circular DNA are depicted. The encapsidated rcDNA might be shuttling back to the nucleus to refill the cccDNA pool. (**B**) Schematic Southern blot pattern derived from highly HBV-infected samples depicting a typical picture with major bands. The blot is labelled on the right-hand side with HBV DNA forms that are present in the respective bands or smears.

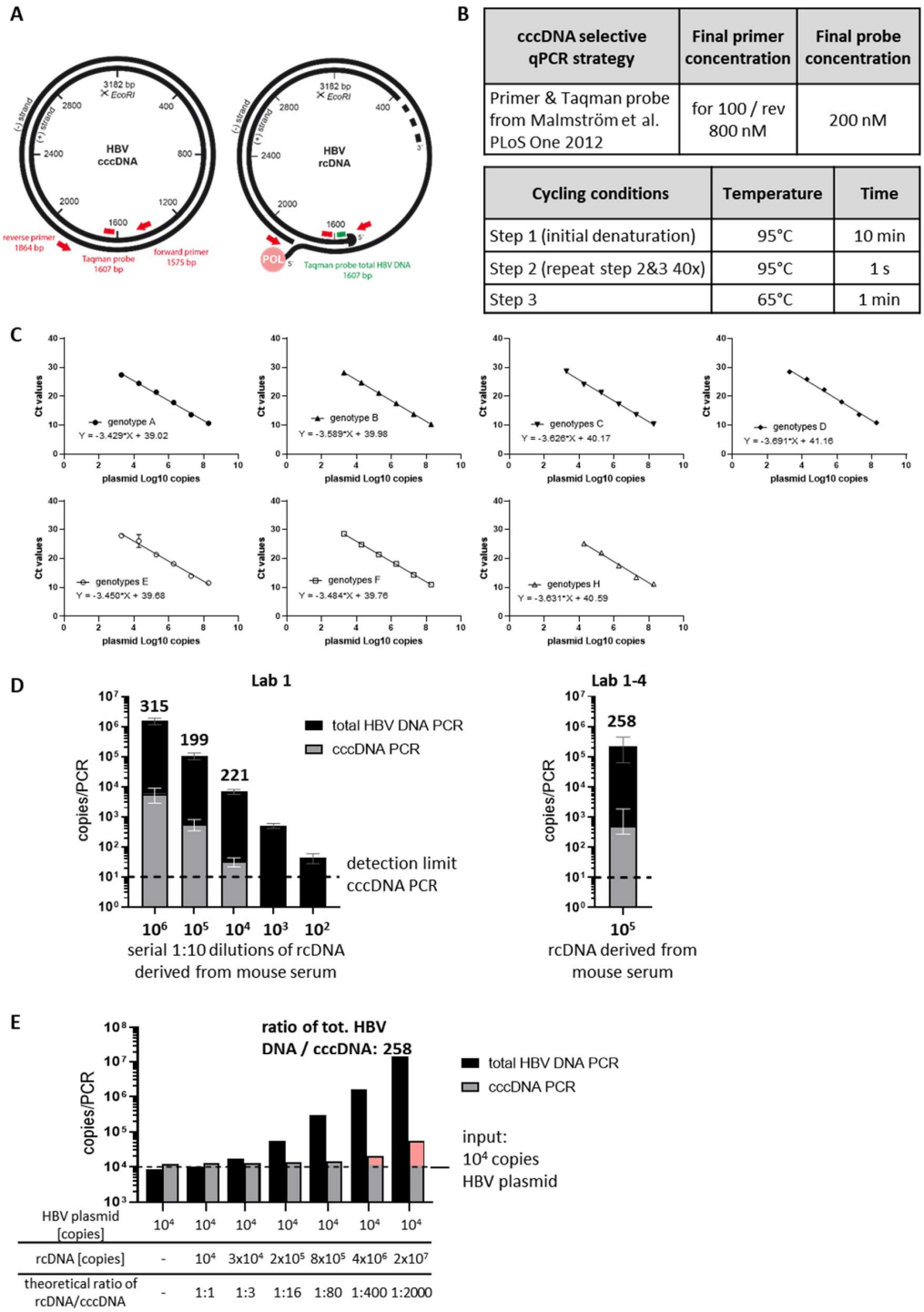

cccDNA selective qPCR strategy	Final primer concentration	Final probe concentration
Primer & Taqman probe from Malmström et al. PLoS One 2012	for 100 / rev 800 nM	200 nM

Cycling conditions	Temperature	Time
Step 1 (initial denaturation)	95°C	10 min
Step 2 (repeat step 2&3 40x)	95°C	1 s
Step 3	65°C	1 min

HBV plasmid [copies]	10^4	10^4	10^4	10^4	10^4	10^4	10^4
rcDNA [copies]	-	10^4	$3x10^4$	$2x10^5$	$8x10^5$	$4x10^6$	$2x10^7$
theoretical ratio of rcDNA/cccDNA	-	1:1	1:3	1:16	1:80	1:400	1:2000

Supplementary figure 2: Characterization of the cccDNA-selective qPCR strategy used in this study. (**A**) A schematic presentation of the primer and probe binding sites on cccDNA and rcDNA is shown in red. The binding site of the probe for the qPCR detecting total HBV DNA is shown as a green dash. (**B**) The table summarizes the qPCR conditions for the cccDNA-selective PCR used throughout the study. (**C**) This qPCR strategy detects all HBV genotypes except genotype G with comparable efficiencies. Serial dilutions of plasmids each containing

the consensus sequence built from the HBVdb database (https://hbvdb.lyon.inserm.fr/HBVdb/) for every genotype were run in triplicates and the standard curve was computed. (**D**) rcDNA derived from two mice was analyzed by qPCR for cccDNA (grey bars) and total HBV DNA (black bars) showing the median and range. The false detection ratio (determined by the total HBV DNA copy number divided by the copy number detected by the cccDNA-selective PCR) is depicted on top of the bars and was around 250 indicating that rcDNA is amplified in the cccDNA-selective PCR in a false-positive manner with a ratio of 1:250. The PCR strategy was implemented in every lab and showed comparable cccDNA specificity in serum-derived rcDNA. (**D**) A fixed amount of an HBV containing plasmid (10^4 copies/per reaction) was mixed with increasing concentration of mouse serum derived rcDNA as indicated below the graph. Liver DNA from an uninfected USG mouse was included in every reaction to simulate conditions in actual infectious liver samples. These artificial mixtures were analyzed by qPCR for cccDNA (grey bars) and total HBV DNA (black bars). Red color indicates the fraction of cccDNA counts that is detected in a false-positive manner. The number on top of the bar depicts the false detection ratio (i.e. total HBV DNA copy numbers / cccDNA copy numbers) in this sample. This experiment illustrates the effect of this false-positive detection in mixtures of an HBV plasmid (as a surrogate for cccDNA) and increasing amounts of serum-derived rcDNA mimicking the situation in infected samples. When rcDNA levels exceed HBV DNA plasmid levels by more than 250 fold, measured cccDNA levels increase due to the false-positive detection of rcDNA and a precise quantification of cccDNA is not possible.

A

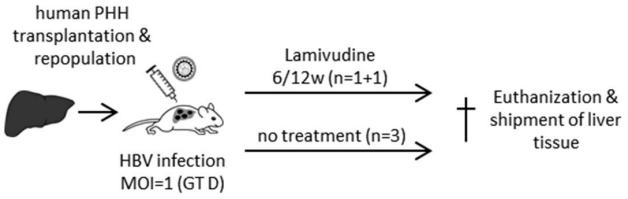

B

Treatment	Usage in study	Viral loads in serum at BL [HBV DNA copies/mL]	Viral loads in serum at EoT [HBV DNA copies/mL]	Log10 reduction to baseline
untreated control	cross-validation (Fig. 1 & 2A, B)	7.3E+08		
untreated control	parallel SB & qPCR (Fig. 2D)	9.1E+08		
untreated control	preparative gel (Fig. 3) & alkaline Hirt (Fig. S5)	6.8E+09		
6w Lamivudine	preparative gel (Fig. 3) & alkaline Hirt (Fig. S5)	1.9E+09	1.7E+07	2.1
12w Lamivudine	preparative gel (Fig. 3) & alkaline Hirt (Fig. S5)	3.1E+09	9.7E+06	2.5

C

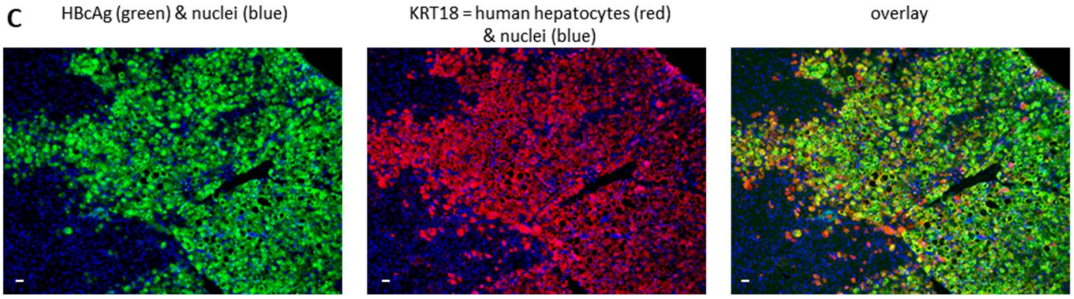

Supplementary figure 3: Sample preparation and virological characterization. (**A**) Schematic presentation of the generation and treatment of humanized liver chimeric mice used in this study. (**B**) The table summarizes the mice, their usage for the presented experiments, their final HBV DNA titers in the serum and, where applicable, their titer at the end of treatment and reductions from baseline. (**C**) Immunofluorescence co-staining for HBV core antigen (green) and the cytokeratin 18 (KRT18) in red as a marker for human hepatocytes in cryopreserved liver sections. Nuclei were stained with Hoechst 33258 (blue). Scale bar = 50 µm; BL, baseline; EoT; end of treatment.

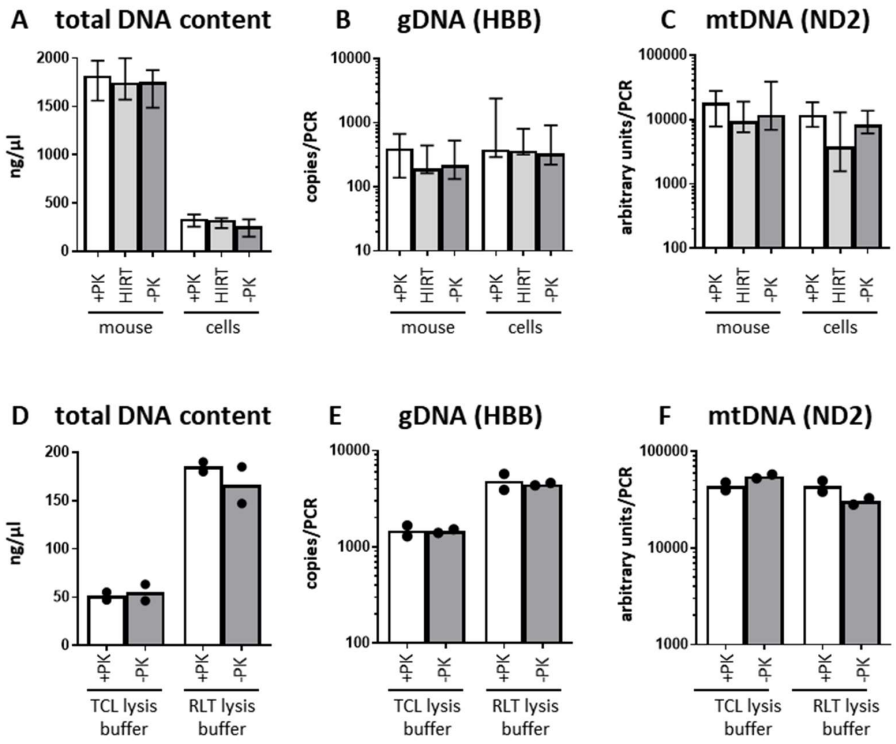

Supplementary Figure 4: The DNA extraction protocol affects the recovery of different types of DNA which in turn influences the normalization strategy. (**A-C**) The recovery of total DNA (measured by spectrophotometry) (**A**), genomic DNA (measured by qPCR for the human single-copy gene HBB) (**B**), and mitochondrial DNA (measured by qPCR for the human mitochondrial gene ND2) (**C**) are depicted as bar graphs for the three tested extractions and the two type of samples as indicated below the graphs. The bars show the median and range of the measurements in four labs. (**D-F**) The total DNA extraction with and without proteinase K treatment was tested head-to-head with the proprietary TCL buffer (Epicentre) and an alternative lysis buffer RLT (Qiagen) using two HBV-infected, untreated humanized mice. Every dot depicts one mouse, the bars the mean. The recovery of total DNA was measured by fluorometry (**D**), genomic DNA by qPCR for the human single-copy gene HBB (**E**), and mitochondrial DNA by qPCR for the human mitochondrial gene ND2 (**F**). gDNA, genomic DNA; HBB, hemoglobin subunit beta; mtDNA, mitochondrial DNA; ND2, mitochondrially encoded NADH:ubiquinone oxidoreductase core subunit 2.

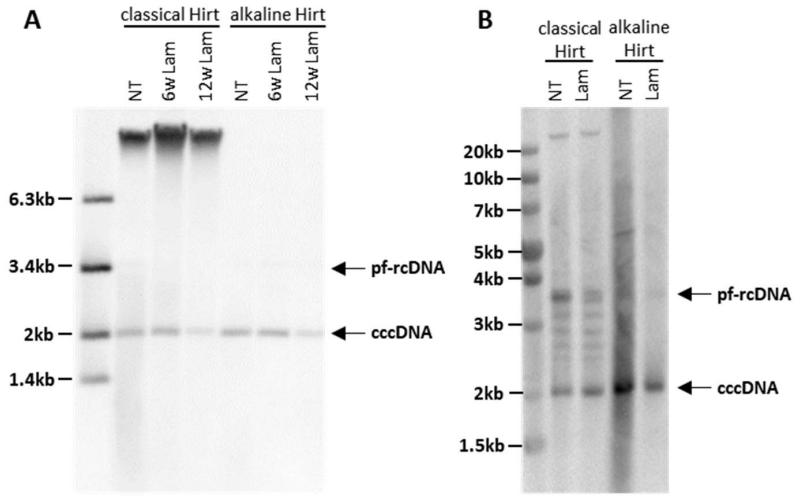

Supplementary Figure 5: Side-by-side comparison of classical and alkaline Hirt procedures. DNA was extracted with the alkaline and the classical Hirt method and subjected to SB as described in Supplementary Materials and Methods. (**A**) Liver DNA from three stably HBV-infected USG mice (after six or 12 weeks of Lamivudine treatment, or untreated, same mice as in **Figure 3**). (**B**) DNA from HepG2-NTCP cells infected with HBV (HepAD38-derived virus at MOI 250 GE / cell) and cultured for 9 days with or without Lamivudine treatment (10uM). In contrast to the classical method, cells are lysed in an alkaline milieu leading to the irreversible denaturation of genomic DNA and all non-supercoiled HBV DNA species, which are removed by centrifugation after rapid neutralization. As can be seen on the upper part of the blot, genomic DNA is visible only in the classical Hirt DNA extracts, confirming the higher capacity of alkaline extraction to deplete it. However, qPCR for HBB as an indicator of genomic DNA showed that genomic DNA was still present to varying extents (data not shown). In cell culture derived samples (**B**), most of the slow-migrating, relaxed HBV DNA forms, as well as “T5-resistant forms” (see **Supplementary Fig. 7**) are absent in the alkaline Hirt DNA extracts. These forms are not detected in either classical or alkaline Hirt extracts of mice livers (**A**), probably due to sensitivity issues or the high quality of the obtained DNA, i.e. no contribution of nicked cccDNA to the slow-migrating upper band. A smear in the alkaline Hirt-derived sample is visible in cell culture extracts (**B**, lane 4), which is absent under Lamivudine treatment (lane 5), suggesting that it is specific to HBV DNA. Lam, Lamivudine; NT, non-treated.

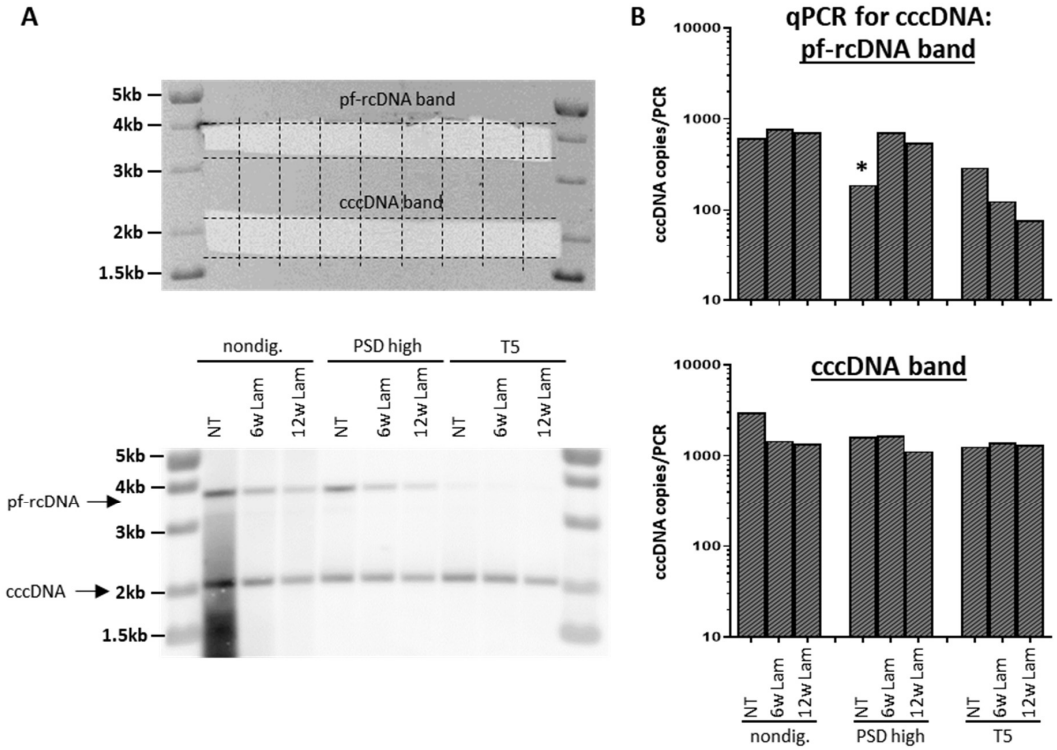

Supplementary Figure 6: The pf-rcDNA is detected with the same efficiency as cccDNA by cccDNA-selective qPCR. (**A**) The upper and lower bands of a parallel gel (same samples as in Figure 3) were excised separately and the DNA was extracted. The top photographs shows the agarose gel after excision; the lower photograph shows the parallel SB for comparison. (**B**) The upper graph depicts qPCR measurements for cccDNA in samples originating from the upper band in copies / PCR assay. The lower graph depicts the measurements from the lower band. The asterisk (*) marks a sample where some of the material was lost during the gel extraction process. Lam, Lamivudine; NT, non-treated.

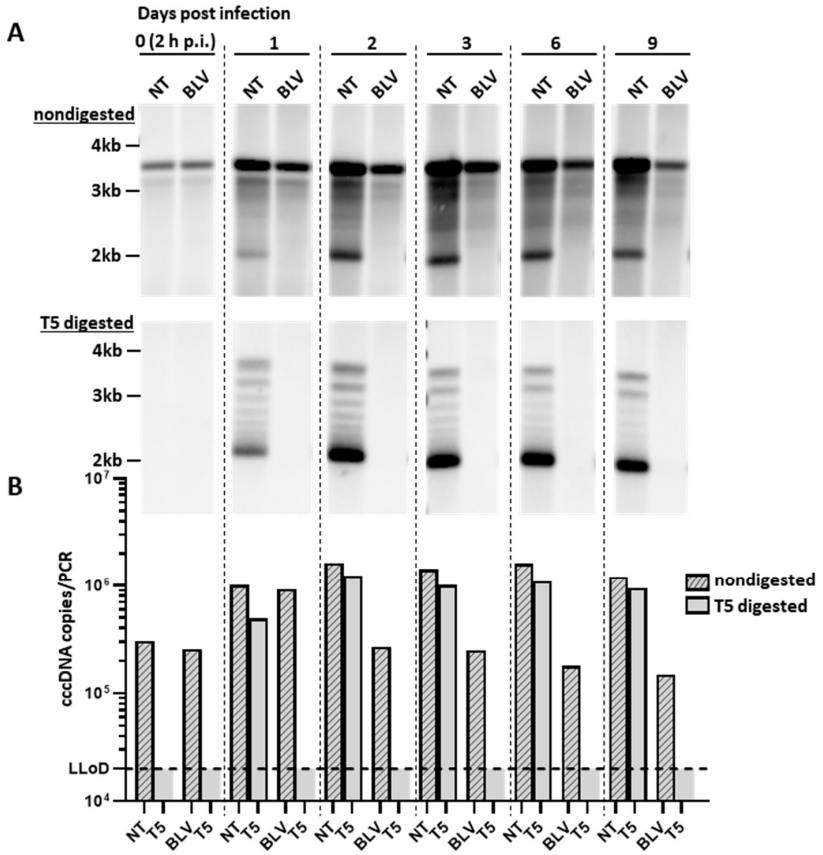

Supplementary figure 7: Persistent pf-rcDNA from input virus interferes with cccDNA measurements in cell culture but can be removed by T5 exonuclease treatment. (**A, B**) HepG2-NTCP cells were infected with HBV (HepAD38-derived virus at MOI 4000 GE / cell) and followed up for nine days in the presence of Bulevirtide (185 nM) or without treatment. Hirt DNA was extracted at the indicated time points and subjected to SB (**A**) and cccDNA-selective qPCR (**B**) analyses either without additional nuclease digestion or after T5 exonuclease digestion. Samples treated with T5 exonuclease are shown in the bottom blot or with hatched bars, respectively. On the bottom blot, twice as much DNA as on the top blot was loaded. BLV, Bulevirtide; NT, non-treated.

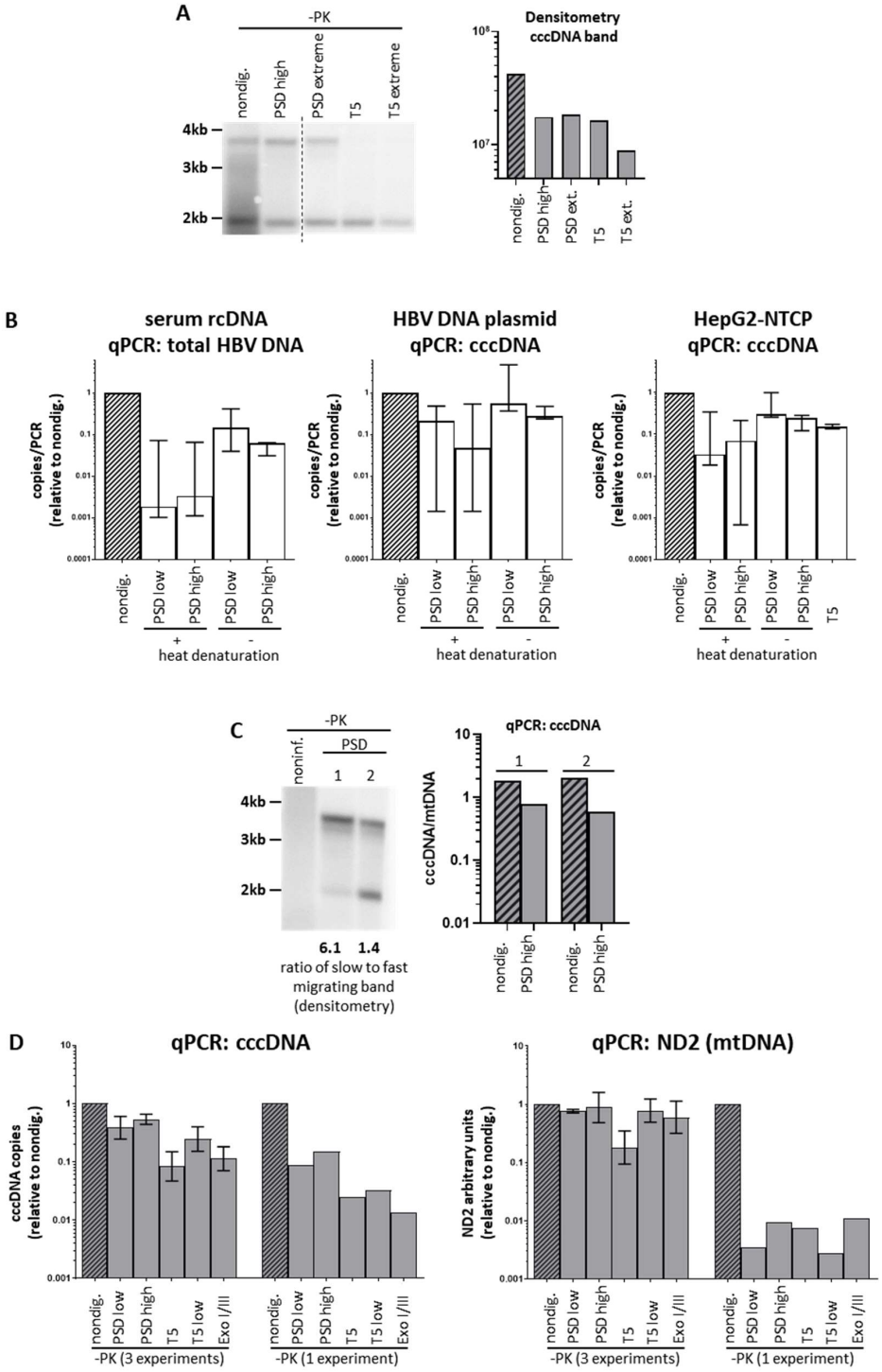

Supplementary Figure 8: Nuclease treatment bears the risk of over-digesting cccDNA when digestion conditions are exaggerated or when the input DNA is damaged. (**A**) SB analysis (left) and densitometry of the cccDNA band (right) of -PK extracted liver DNA from one stably infected untreated USG mouse after various nuclease treatments. The standard conditions for PSD and T5 were compared to extreme conditions: “PSD high”: 30 U PSD in 200 µl, 2 h incubation vs. “PSD extreme”: 120 U PSD in 200 µl, 6 h incubation and “T5”: 10 U T5

exonuclease in 20 µl; 45 min incubation vs “T5 extreme”: 40 U T5 exonuclease in 20 µl; 6 h incubation. Note that the higher band volume of the nondigested sample determined by densitometry is due excessive background staining in this lane. (**B**) Comparison of PSD digestion efficiency with and without prior heat denaturation of the input DNA. DNA from HepG2-NTCP cells was extracted with the +PK extraction protocol. Serum rcDNA was extracted from humanized mouse serum using the QiAamp MinElute Virus Spin Kit. Extracted rcDNA and purified HBV DNA plasmid was diluted in +PK extracted DNA from an uninfected humanized mouse before nuclease digestion. The bar graphs show total HBV DNA or cccDNA copy numbers normalized to the nondigested levels. Bars depict the median and range of measurements from four labs. The sample type and qPCR are depicted above the respective graphs. (**C**) SB analysis (left) and qPCR for cccDNA (right) in two individual -PK DNA extracts from the same untreated HBV-infected USG mouse (denoted as 1 and 2). The ratio of upper and lower band was determined by densitometry. qPCR measurements of cccDNA normalized to mitochondrial DNA via ND2 are shown beside the blot before and after nuclease digestion. (**D**) qPCR measurements of cccDNA and ND2 in -PK extracted liver DNA from an HBV-infected USG mouse liver tissue, digested with nucleases as indicated below the graph or left undigested (hatched bars) The left-hand side of each graph shows three independent DNA extraction; the right-hand side shows the results of a failed -PK DNA extraction in one experiment, which resulted in damaged DNA. Bars depict the median of three experiments. Copy numbers per qPCR assay were normalized to the values in the nondigested sample.

Supplementary references

1. Allweiss L, Volz T, Giersch K, et al. Proliferation of primary human hepatocytes and prevention of hepatitis B virus reinfection efficiently deplete nuclear cccDNA in vivo. Gut 2017.

2. Ko C, Chakraborty A, Chou W-M, et al. Hepatitis B virus genome recycling and de novo secondary infection events maintain stable cccDNA levels. J Hepatol 2018;69:1231–1241.

3. Stadelmayer B, Diederichs A, Chapus F, et al. Full-length 5'RACE identifies all major HBV transcripts in HBV-infected hepatocytes and patient serum. J Hepatol 2020.

4. Zhang YY, Summers J. Low dynamic state of viral competition in a chronic avian hepadnavirus infection. J Virol 2000;74:5257–5265.

5. Suslov A, Meier M-A, Ketterer S, et al. Transition to HBeAg-negative chronic hepatitis B virus infection is associated with reduced cccDNA transcriptional activity. J Hepatol 2021;74:794–800.

6. Werle-Lapostolle B, Bowden S, Locarnini S, et al. Persistence of cccDNA during the natural history of chronic hepatitis B and decline during adefovir dipivoxil therapy. Gastroenterology 2004;126:1750–8.

7. Xia Y, Stadler D, Ko C, et al. Analyses of HBV cccDNA Quantification and Modification. Methods Mol Biol Clifton NJ 2017;1540:59–72.

8. Long Q, Yan R, Hu J, et al. The role of host DNA ligases in hepadnavirus covalently closed circular DNA formation. PLoS Pathog 2017;13:e1006784.

9. Qu B, Ni Y, Lempp FA, et al. T5 Exonuclease Hydrolysis of Hepatitis B Virus Replicative Intermediates Allows Reliable Quantification and Fast Drug Efficacy Testing of Covalently Closed Circular DNA by PCR. J Virol 2018;92.

10. Hu J, Protzer U, Siddiqui A. Revisiting Hepatitis B Virus: Challenges of Curative Therapies. J Virol 93:e01032-19.

11. Luo J, Cui X, Gao L, et al. Identification of an Intermediate in Hepatitis B Virus Covalently Closed Circular (CCC) DNA Formation and Sensitive and Selective CCC DNA Detection. J Virol 2017;91.

12. Jiang P-X, Mao R-C, Dong M-H, et al. Exonuclease I and III improve the detection efficacy of hepatitis B virus covalently closed circular DNA. Hepatobiliary Pancreat Dis Int HBPD INT 2019;18:458–463.

13. Malmstrom S, Larsson SB, Hannoun C, et al. Hepatitis B viral DNA decline at loss of HBeAg is mainly explained by reduced cccDNA load--down-regulated transcription of PgRNA has limited impact. PLoS One 2012;7:e36349.

14. Allweiss L, Giersch K, Pirosu A, et al. Therapeutic shutdown of HBV transcripts promotes reappearance of the SMC5/6 complex and silencing of the viral genome in vivo. Gut 2021.

15. Lebossé F, Inchauspé A, Locatelli M, et al. Quantification and epigenetic evaluation of the residual pool of hepatitis B covalently closed circular DNA in long-term nucleoside analogue-treated patients. Sci Rep 2020;10:21097.

16. Niu C, Livingston CM, Li L, et al. The Smc5/6 Complex Restricts HBV when Localized to ND10 without Inducing an Innate Immune Response and Is Counteracted by the HBV X Protein Shortly after Infection. PLoS One 2017;12:e0169648.